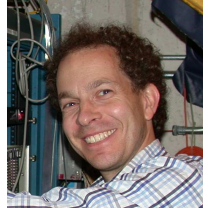


Recent Spin Results from STAR

Andrew Gordon for the STAR Collaboration
*Department of Physics, Brookhaven National Laboratory,
 20 Pennsylvania Street, Upton, NY*



In Run 8 at RHIC, STAR significantly enhanced its forward acceptance relative to previous years with the commissioning of a new detector, the Forward Meson Spectrometer (FMS). The large geometrical acceptance of the FMS allows us to extend the forward reach of the data beyond inclusive pions accessed by modular calorimeters. The spin-1 ω is accessible to the FMS through its decay channel $\omega \rightarrow \pi^0 \gamma$. Such events can help disentangle the dynamical origins of observed large analyzing powers in the forward region, and can contribute to our knowledge of the nuclear medium by comparisons of p+p to d+Au. Here we report on the status of this analysis.

1 Introduction

The fundamental goal of the spin program at STAR is to determine how the proton acquires spin from its constituent quarks and gluons. This program makes use of both longitudinally and transversely polarized p+p collisions at Brookhaven National Laboratory's Relativistic Heavy Ion Collider (RHIC). The longitudinal data has allowed STAR to put strong constraints on the contribution of the gluon spin, down to x-Bjorken ~ 0.02 .^{1,2}

Run 8 at RHIC, which ran during the Fall and Winter of 2007/2008 and finished in the Spring of 2008, included both d+Au collisions at $\sqrt{s_{NN}} = 200$ GeV, as well as transversely polarized p \uparrow + p \uparrow collisions at $\sqrt{s} = 200$ GeV. Important goals of Run 8 were to provide measurements of the low-x gluon density in the nucleon, to search for the onset of gluon saturation effects through intercomparisons of $\pi^0 \pi^0$ data between p+p and d+Au collisions, and to further characterize the significant single spin asymmetries that have been observed in the forward region.^{3,4}

Consistent with these goals, STAR commissioned a new detector for Run 8, the Forward Meson Spectrometer (FMS).⁵ The FMS is a nearly hermetic array of 1264 lead-glass blocks ("cells") situated ~ 700 cm downstream of the interaction point and spanning an area 200×200 cm² perpendicular to the beam pipe. It covers the full azimuth in the range $2.5 < \eta < 4.0$ and provides a many-fold increase in the areal coverage of the forward region at STAR.⁵

STAR has previously reported on precision measurements⁴ of the analyzing power (A_N) of inclusive neutral pions in the forward region. These measurements used data taken in RHIC runs 3, 5, and 6 with the Forward Pion Detector (FPD), a modular lead-glass array which can be moved horizontally in the plane transverse to the beamline. These data were taken at $\sqrt{s} = 200$ GeV, where inclusive π^0 cross sections are consistent with expectations from pQCD.⁶ The measurements showed that the variation of A_N with Feynman-x ($X_F = 2P_L/\sqrt{s}$) was qualitatively consistent with expectations from the Sivers effect,⁷ while the P_T dependence was not. Inclusive measurements of η asymmetries have also been reported.⁸

The Sivers effect identifies the origin of the observed spin asymmetries with orbital motion of the quarks inside the polarized proton. This leads to a correlation between the proton spin and the intrinsic transverse momentum of the struck quark in the hard scatter, which then manifests itself as a Left/Right asymmetry in the resulting jet direction. By contrast, in the Collins effect^{9,10} the polarization of the struck quark is correlated to the polarization of the proton, and the fragmentation of the polarized quark leads to Left/Right asymmetries within the resulting jet. It remains to be determined the extent to which these two effects contribute to the observed single spin asymmetries.⁵

Forward jet data can help separate the two contributions. Jet measurements that integrate the full azimuth about the jet thrust axis could lead to Sivers-type asymmetries, while jet measurements that depend on the azimuth about the thrust axis could lead to Collins asymmetries. The Run 8 FMS data were accumulated with a “high tower” trigger, in which a single lead-glass detector was required to have energy above a threshold to trigger event acquisition. This tends to bias the data towards jets for which a few electromagnetic particles account for the bulk of the fragmentation, and PYTHIA¹¹ studies have demonstrated that we expect most of the energy in these jets to derive from only a few fragmentation products. Simulation studies also show resonance peaks within the observed jet clusters.

The inclusive pions tend to originate from various resonances along the fragmentation decay chain, and we have begun to study resonances heavier than neutral pions as a first step towards understanding jet data. One source of neutral pions is the isoscaler, spin-1 ω through the decay channel $\omega \rightarrow \pi^0\gamma$ (BR=8.9%¹²). For this resonance, A_N measurements can provide crucial information for the Collins effect. The Collins effect is consistent with string fragmentation models in which a quark/anti-quark pair is produced with relative orbital angular momentum at the point of string breaking.^{13,14} This leads to a Left/Right asymmetry for the production of the spin 0 pions, and would lead to the opposite asymmetry for the spin 1 ω . Direct observation of a negative A_N might provide strong evidence for the Collins effect.

Finally, there are theoretical expectations that a dense hadronic medium produces a partial restoration of chiral-symmetry. An observable impact of this would be shifts in the spectral properties (e.g. mass and width) of the light vector mesons.^{15,16} An analysis of data from PHENIX showed no shift in the ω mass relative to the π^0 , although the analysis only analyzed central particles and was sensitive down to a minimum P_T of 2.5 GeV.¹⁷ The d+Au data from Run 8 can potentially allow us to extend this measurement to higher rapidities and lower P_T .

Here we report on initial observations of an ω signal in the Run 8 p+p data in the FMS.

2 Data and Simulation

The FMS data are clustered, and each cluster is fit to a photon shower shape to determine transverse position and energy. The conversion gains of each cell are determined from π^0 mass peaks through an iterative procedure, and these gains have been shown to be stable over the run at the level of a few percent. A full PYTHIA(6.222) + GEANT simulation has been developed,⁵ and a comparison of data and simulation is shown in Figure 1 for the invariant mass of all pairs of clusters in an event, for minimum bias data. A pronounced π^0 mass peak is evident, and data

and simulation agree well over a large range.

Decays of the spin 1, 782 MeV ω are accessible to the FMS through the decay channel $\omega \rightarrow \pi^0 \gamma$. For this decay, two of the photon clusters derive from the π^0 decay and one directly from the ω . For each triple of clusters there are three possible pairs that can be associated with the π^0 decay. We form the invariant mass of each, and the pair whose mass is closest to 0.135 GeV/c² is associated with the π^0 decay. Simulations show that this procedure tags the photons correctly upwards of 99% of the time.

To help reduce backgrounds we apply relatively high thresholds in both energy and P_T . We consider all triples for which each cluster has energy above 6 GeV, $|\vec{P}_T(\text{triple})| > 2.5$ GeV/c, and $E(\text{triple}) > 30$ GeV. We also require that $P_T > 1.5$ GeV/c for the cluster associated with the ω decay photon. For the two clusters associated with the ω decay pion, we require that their mass be within 0.1 of 0.135 GeV/c² and that $|\vec{P}_T(\pi^0)| > 1$ GeV/c.

Figure 2 shows the mass of all cluster pairs associated with the pion in each triple, and a π^0 peak is evident.

The mass of all triples is shown in Figure 3. An ω peak of roughly 10 statistical standard deviations is evident. The PYTHIA(6.222) + GEANT simulation is shown overlaid on the data. The simulation overpredicts the data at low mass and underpredicts at high mass. Interestingly, we also observe a discrepancy in the distribution (data not shown) of the quantity $\Delta\phi \equiv \phi(\pi^0) - \phi(\gamma)$, where $\phi(\pi^0)$ is the azimuth of the two clusters associated with the ω decay pion and $\phi(\gamma)$ the azimuth of the decay photon. Both simulation and data show a single peak at 0, but the RMS for the simulation is significantly narrower than the data (0.616 ± 0.020 radians for PYTHIA(6.222) + GEANT compared to 0.827 ± 0.003 for the data, a difference of ~ 10 statistical standard deviations). To test that $\Delta\phi$ is driving the discrepancy in the mass, we weighted the simulation by the ratio of data and simulation $\Delta\phi$ histograms. The resulting mass distribution (shown in Figure 3) agrees well with the data.

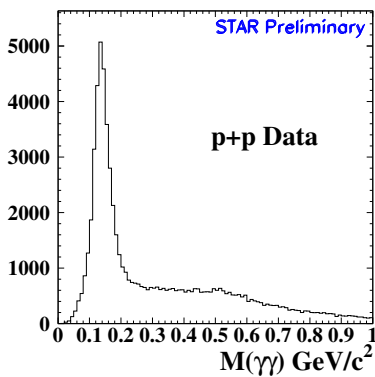


Figure 2: Mass of the two clusters in each triple associated with the ω decay π^0 , without π^0 mass cut.

($\sim 55 \pm 10\%$) are events where the three clusters derive from the decays of two neutral pions. The next source ($\sim 30 \pm 10\%$) are events that contain both an $\eta \rightarrow \gamma\gamma$ decay and a π^0 decay. There are also small contributions from fragmentation photons as well as other backgrounds. We note that π^0 decay photons tend to be near each other at the FMS, and the $\pi^0\pi^0$

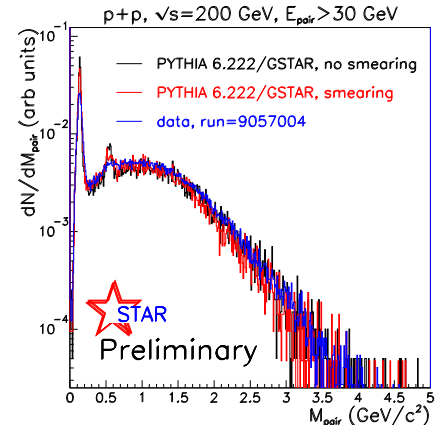


Figure 1: Mass of all pairs with $E > 2$ GeV for p+p data (blue), GEANT simulation (black, labeled “GSTAR”), and for GEANT+additional smearing (red). The additional smearing is ~ 10 MeV, as determined from the π^0 peak in high-tower associated mass distributions.

To confirm that the $\Delta\phi$ discrepancy is not caused by our detector simulation, we removed the GEANT simulation and replaced it with simple geometrical acceptance cuts. We then examined all PYTHIA photons, treating each as a separate, perfectly measured electromagnetic cluster. This new $\Delta\phi$ distribution has an RMS of 0.624 ± 0.006 , consistent with the full simulation. We also examined the PYTHIA parameters of “CDF Tune A,”¹⁸ but saw no significant change, while changing to PYTHIA version 6.420 produced an even narrower peak. We conclude that the distribution of momentum components perpendicular to the thrust axis (j_T) can be tuned in PYTHIA and requires better tuning in the forward region.

To understand the backgrounds, we examine the PYTHIA event record for each event in the ω mass region ($0.68 < M(\text{triple}) < 0.88$ GeV/c²). The largest background in this re-

background can be reduced by cuts on the smallest transverse distance at the FMS between the ω photon and any cluster in the event that is not part of the triple being analyzed.

3 Conclusion

The FMS was newly commissioned for Run 8. The detector has been calibrated, and a rich data set has begun to be analyzed. We have reported on an analysis of three-cluster events in the FMS, with a goal to extract measurements of asymmetries of the spin-1 ω , as well as to compare its spectral properties between p+p and d+Au data. The ω signal is readily visible in the p+p data, with a statistical significance of roughly 10σ . However, the signal to noise level is currently insufficient to extract A_N , and future work will focus on attempts to reduce the background level.

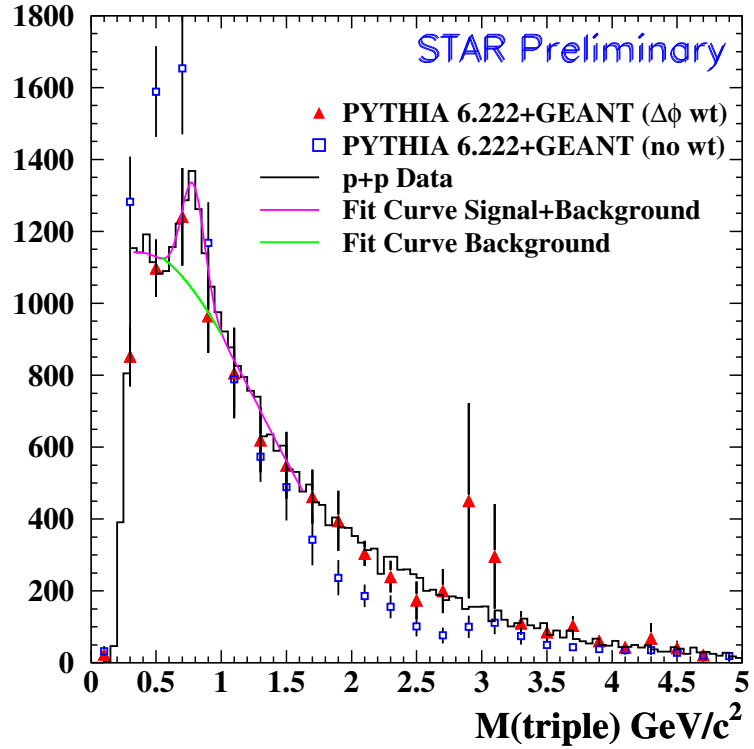


Figure 3: Mass of all triples for data (black solid), PYTHIA + GEANT (blue squares), and weighted PYTHIA + GEANT (red triangles, see text). Simulation is normalized to data. A gaussian+cubic polynomial fit is overlaid (magenta curve). The fit gaussian mean and width are $\mu = 0.784 \pm 0.008 \text{ GeV}/c^2$ and $\sigma = 0.087 \pm 0.009 \text{ GeV}/c^2$, and the fitted total area under the Gaussian is 1339 ± 135 events. The cubic background shape is also shown (green curve).

References

1. B.I. Abelev et al, *Phys. Rev. Lett.* **100**, 232003 (2008).
2. B.I. Abelev et al, *Phys. Rev. Lett.* **97**, 252001 (2006).
3. L.C. Bland et al, *Eur. Phys. J. C* **43**, 427 (2005).
4. B.I. Abelev et al, *Phys. Rev. Lett.* **101**, 222001 (2008).
5. N. Poljak, *arXiv:0901.2828* proc. SPIN 2008, Charlottesville, Virginia, to be published.
6. J. Adams et al, *Phys. Rev. Lett.* **97**, 152302 (2006).
7. D. Sivers, *Phys. Rev. D* **41**, 93 (1990).
8. S. Heppelmann, proc. PANIC 2008, Eilat, Israel, to be published.
9. J. C. Collins, *Nucl. Phys. B* **396**, 161 (1993).
10. J. Collins, S. Heppelmann, G. Ladinsky, *Nucl. Phys. B* **420**, 565 (1994).
11. T. Sjöstrand et al, *Computer Phys. Commun.* **135**, 238 (2001); *hep-ph/0010017*.
12. W.-M. Yao et al. (Particle Data Group), *J. Phys. G* **33**, 1 (2006).
13. X. Artru and J. Czyżewski, H. Yabuki, *hep-ph/9508239v1* (1995).
14. X. Artru and J. Czyżewski, *hep-ph/9805463v1* (1998).
15. G.E. Brown and M. Rho, *Phys. Rev. Lett.* **66**, 21 (1991).
16. R. Rapp and J. Wambach, *Adv. Nucl. Phys.* **25**, 1 (2000); *hep-ph/9909229*.
17. S.S. Adler et al, *Phys. Rev. C* **75**, 051902(R) (2007).
18. R. Field, *Min-Bias and the Underlying Event at the Tevatron and the LHC*, talk presented at the Fermilab ME/MC Tuning Workshop, Fermilab, October 4, 2002.